Opsonization-Enhanced Antigen Presentation by MR1 Activates Rapid Polyfunctional MAIT Cell Responses Acting as an Effector Arm of Humoral Antibacterial Immunity

Caroline Boulouis,* Jean-Baptiste Gorin,* Joana Dias,* Peter Bergman,[†,‡] Edwin Leeansyah,*[,§] and Johan K. Sandberg*

Mucosa-associated invariant T (MAIT) cells are innate-like antimicrobial T cells recognizing a breadth of important pathogens via presentation of microbial riboflavin metabolite Ags by MHC class Ib–related (MR1) molecules. However, the interaction of human MAIT cells with adaptive immune responses and the role they may play in settings of vaccinology remain relatively little explored. In this study we investigated the interplay between MAIT cell–mediated antibacterial effector functions and the humoral immune response. IgG opsonization of the model microbe *Escherichia coli* with pooled human sera markedly enhanced the capacity of monocytic APC to stimulate MAIT cells. This effect included greater sensitivity of recognition and faster response kinetics, as well as a markedly higher polyfunctionality and magnitude of MAIT cell responses involving a range of effector functions. The boost of MAIT cell responses was dependent on strongly enhanced MR1-mediated Ag presentation via increased FcγR-mediated uptake and signaling primarily mediated by FcγRI. To investigate possible translation of this effect to a vaccine setting, sera from human subjects before and after vaccination with the 13-valent–conjugated *Streptococcus pneumoniae* vaccine were assessed in a MAIT cell activation assay. Interestingly, vaccine-induced Abs enhanced Ag presentation to MAIT cells, resulting in more potent effector responses. These findings indicate that enhancement of Ag presentation by IgG opsonization allows innate-like MAIT cells to mount a faster, stronger, and qualitatively more complex response and to function as an effector arm of vaccine-induced humoral adaptive antibacterial immunity. *The Journal of Immunology*, **2020, 205: 67–77.**

Mucosa-associated invariant T (MAIT) cells belong to the family of unconventional T cells that share the ability to recognize nonprotein Ags presented by MHC class I–like molecules (1–4). MAIT cells have a systemic presence in humans and are particularly abundant in mucosal barrier tissues and in the liver (5–7). MAIT cells express a semi-invariant αβ TCR (8–10) and recognize microbial metabolite Ags derived from the vitamin B2 biosynthesis pathway shared by many microbes, presented by the MHC class Ib–related (MR1) molecules (11, 12). When activated by such Ags, they respond in a rapid, innate-like manner with release of cytokines, including IFN-γ, TNF, and IL-17 (5, 13), and mediate cytolytic effector functions against bacteria-infected cells (14–16). Their innate-like T cell response pattern depends on a transcriptional profile characterized by the coexpression of promyelocytic leukemia zinc finger (PLZF) and retinoid-related orphan receptor (ROR) γt (5, 6).

The capacity of MAIT cells to respond to conserved bacterial- and fungal-derived riboflavin metabolites is important for protection against microbial infections, in particular, bacterial infections of the lung (17). This includes immunity against mycobacteria in humans and mice (13, 18, 19) as well as clear protective effects in murine models of *Klebsiella pneumoniae* (20), *Francisella tularensis* (21, 22), and *Legionella longbeachae* infections (23). From an immune homeostasis perspective, it is interesting that mice deficient in MR1, thus lacking MAIT cells, display signs of impaired intestinal integrity and increased microbial translocation (24). Thus, MAIT cells are positioned and poised to respond to microbial infection at mucosal surfaces.

MR1 is highly evolutionarily conserved in mammals, largely nonpolymorphic in humans, and widely expressed intracellularly in many cell types (25–27). MR1 Ag loading occurs in the endoplasmic reticulum (ER), where MR1 is present in a preformed conformation (28). The unstable antigenic metabolite 5-(2-oxoethylideneamino)-6-D-ribitylaminouracil stabilizes MR1 through formation of a covalent Schiff base bond (11, 12), and the stable MR1–5-(2-oxoethylideneamino)-6-D-ribitylaminouracil complex then translocates to the cell surface (28). Thus, in the context of infection, MR1 can be detected at high levels on the surface of

*Center for Infectious Medicine, Department of Medicine, Karolinska Institutet, 14152 Stockholm, Sweden; [†]Division of Clinical Microbiology, Department of Laboratory Medicine, Karolinska Institutet, Huddinge, 14152 Stockholm, Sweden; [‡]Infectious Disease Clinic, Immunodeficiency Unit, Karolinska University Hospital, Huddinge, 14186 Stockholm, Sweden; and [§]Program in Emerging Infectious Diseases, Duke-National University of Singapore Medical School, 169587 Singapore

ORCIDs: 0000-0003-0562-5395 (C.B.); 0000-0003-3306-3713 (P.B.); 0000-0003-0505-4967 (E.L.); 0000-0002-6275-0750 (J.K.S.).

Received for publication January 2, 2020. Accepted for publication April 30, 2020.

This work was supported by grants to J.K.S. from the Swedish Research Council (2016-03052), the Swedish Cancer Society (CAN 2017/777), the Swedish Heart-Lung Foundation (20180675), the Karolinska Institutet Center for Innovative Medicine (20190732), the Karolinska Institutet, and the U.S. National Institute of Diabetes and Kidney Diseases, National Institutes of Health (R01DK108350). Further support to E.L. was from the Swedish Research Council (2015-00174) and Marie Skłodowska Curie Actions, Cofund, Project INCA 600398. J.D. was supported by Fundação para a Ciência e a Tecnologia Doctoral Fellowship SFRH/BD/85290/2012, cofunded by the Programa Operacional Potencial Humano-Quadro de Referência Estratégico Nacional and the European Social Fund.

Address correspondence and reprint requests to Dr. Johan K. Sandberg, Center for Infectious Medicine, Department of Medicine, Karolinska Institutet, Alfred Nobels Allé 8, 14152 Stockholm, Sweden. E-mail address: johan.sandberg@ki.se

The online version of this article contains supplemental material.

Abbreviations used in this article: ER, endoplasmic reticulum; GzB, granzyme B; MAIT, mucosa-associated invariant T; MR1, MHC class Ib–related; OPA, opsonophagocytic activity; PLZF, promyelocytic leukemia zinc finger; ROR, retinoid-related orphan receptor; Syk, spleen tyrosine kinase.

APCs, whereas in the absence of antigenic ligand, the surface expression is generally very low. In addition to direct MAIT cell triggering via recognition of MR1-presented Ags, high expression of the receptors for IL-18 and IL-12 endows MAIT cells with the capacity to respond to these cytokines produced by APCs in response to pattern recognition signals (13). This innate cytokine pathway can enhance TCR-mediated MAIT cell activation (29, 30) and trigger MR1-independent MAIT cell responses (31–34).

Phagocytosis of microbes by APCs can be triggered by lectin- and scavenger receptors (35). Notably, however, Ags from microbes covered by opsonins, such as IgG or complement, are more efficiently endocytosed, processed, and presented to MHC-restricted T cells (36). The activating Fcγ receptors expressed by APCs, including FcγRI (CD64), FcγRIIA/C (CD32A/C), and FcγRIIIA (CD16A), transduce signals through the ITAM located in the cytoplasmic domain of CD32A/C or in the associated FcRγ adaptor protein for CD64 and CD16A (37). Activating signals from FcγRs induce a range of different functions, including microbial phagocytosis and processing for Ag presentation on MHC class I and II (37). Much less is known about the role of FcγRs for Ag processing and presentation by MR1.

Streptococcus pneumoniae is a human pathogen that can cause severe diseases, such as meningitis, bacteremia, and pneumonia (38), with the young and the elderly as the most susceptible populations (39). Naturally acquired immunity to *S. pneumoniae* is dependent on Ab responses to bacterial surface proteins (40). Vaccines that target polysaccharides of *S. pneumoniae* generate IgG-mediated humoral immunity protecting against the serotypes included in the vaccine (41). Interestingly, recent findings indicate that MAIT cells can recognize and mount robust responses to pneumococci via both MR1-dependent and MR1-independent routes (42, 43). Little is known regarding the interplay between the adaptive humoral immune response and the MAIT cell compartment, which is capable of mediating innate-like rapid effector functions. In this study, we investigated this interaction by first dissecting the impact of IgG opsonization on MR1-mediated Ag presentation, the subsequent detection of MR1-restricted Ag by MAIT cells, and the quality of the ensuing MAIT cell response. We next investigated how potentiating effects on all these levels translate into enhanced MAIT cell detection of *S. pneumoniae* in response to vaccination. Altogether, our findings indicate that IgG opsonization of bacteria enhances MR1-mediated Ag presentation, allowing MAIT cells to mount a more efficient and qualitatively different response and to act as an effector arm of humoral vaccine-induced immunity in humans.

Materials and Methods

Human blood samples and tonsil tissue

Peripheral blood was collected from healthy adults recruited at the Blood Transfusion Clinic at the Karolinska University Hospital, Huddinge. Tonsils were collected from patients undergoing tonsillectomy because of sleep disorders in breathing or obstructive sleep apnea syndrome. To isolate cells, the tonsils were cut in small pieces and then smashed mechanically through a 100-μm cell strainer. Mononuclear cells were isolated as described in the *Cell isolation* paragraph. Tonsillectomies were performed at the Department of Otorhinolaryngology at the Karolinska University Hospital, Huddinge or at Cityakuten, Stockholm, Sweden. Written informed consent was obtained from all donors in accordance with study protocols conforming to the provisions of the Declaration of Helsinki and approved by the Regional Ethics Review Board in Stockholm.

Serum samples

Nine healthy donors were recruited by the Immunodeficiency Unit at Karolinska University Hospital, Huddinge (44). Serum was collected from these donors before vaccination and at week 2 or 4 after vaccination with Prevnar13 (pneumococcal 13-valent conjugate vaccine; Pfizer), and data on specific serum IgG titers and opsonophagocytic activity (OPA) collected as described (44). The study was performed in accordance with the Declaration of Helsinki and approved by the Regional Ethics Review Board in Stockholm and by the Swedish Medical Product Agency. The study was registered at www.clinicaltrials.gov as NCT01847781. Written consent was obtained from all subjects prior to inclusion.

Microbes

The *Escherichia coli* strains D21, 1100-2, and the *ribA*-deficient BSV-18 were cultured overnight at 37°C in lysogeny (Luria-Bertani) broth with 3 μg/ml riboflavin supplementation for BSV-18 (45). *S. pneumoniae* 1344 19A was cultured overnight at 37°C and 5% CO_2 in Todd Hewitt Broth. Live microbes were counted by the standard plate counting method on appropriate culture media, and counts were expressed as CFU/ml. The microbes were then stored at −80°C in 50% glycerol/50% FCS for *E. coli* D21 and 50% glycerol/50% PBS for *E. coli* 1100-2, BSV-18, and *S. pneumoniae* 1344 19A. 1100-2 is the congenic strain of BSV-18.

Cell isolation

PBMCs and tonsillar mononuclear cells were prepared by Ficoll-Hypaque density gradient centrifugation (Lymphoprep; Axis-Shield Diagnostics). After isolation, PBMCs and tonsillar mononuclear cells were incubated overnight in RPMI 1640 medium supplemented with 2 mM L-glutamine and 25 mM HEPES (both from Thermo Fisher Scientific) as well as 10% FBS (Sigma-Aldrich), 50 μg/ml gentamicin (Life Technologies), and 100 μg/ml Normocin (InvivoGen). The Vα7.2$^+$ cells were purified from PBMCs and tonsillar mononuclear cells using anti-Vα7.2-PE (BioLegend), followed by positive-selection MACS using anti-PE Microbeads (Miltenyi Biotec).

MAIT cell activation assay

Bacteria were first washed once in PBS, then fixed for 3 min in 1% formaldehyde while being vortexed during the first minutes, and extensively washed in PBS. The bacteria were then resuspended in RPMI 1640 supplemented with 2 mM L-glutamine and 25 mM HEPES (Thermo Fisher Scientific), 50 μg/ml gentamicin (Life Technologies), and 100 μg/ml Normocin (InvivoGen) (no FCS), or incubated with 1, 5, or 10 mg/ml IVIg (GAMUNEX) or 100 μl of pooled serum for 30 min at 37°C. After extensive washes, the microbes were resuspended in medium without FCS and fed to THP-1 monocytic cells at the microbial dose of 1 for *E. coli* and 3 for *S. pneumoniae*. The activation assay was performed as previously described, with slight modification (46). THP-1 cells were seeded in medium without FCS for 2 h prior to adding the bacteria. Vα7.2$^+$ cells and THP-1 were cultured at 2:1 ratio for 24 h in the presence of fixed microbes and 1.25 μg/ml anti-CD28 mAb (L293; BD Biosciences). In all functional assays, MAIT cells were gated and identified by flow cytometry as Vα7.2$^+$CD161$^+$ T cells (46). The THP-1 cell line was maintained in complete medium and routinely tested negative for mycoplasma.

In MR1 blocking experiments, THP-1 cells were preincubated 30 min before adding Vα7.2$^+$ cells with 100 μM acetyl-6-formylpterin (Schircks Laboratories), or anti-MR1 mAb (26.5; BioLegend), or isotype control (MOPC-173; BioLegend) at the final concentration of 20 μg/ml. In IL-12/IL-18 neutralization experiments, THP-1 cells were preincubated 30 min before adding Vα7.2$^+$ cells with anti–IL-12 p40/70 mAb (C8.6; Miltenyi Biotec), anti–IL-18 mAb (125-2H; MBL International) or isotype control (MOPC-21; BioLegend) at the final concentration of 5 μg/ml. In the Fc receptor blocking experiments, THP-1 cells were preincubated 30 min before adding *E. coli* with 20 μg/ml purified Fc fragment from human IgG (Millipore), 10 μg/ml anti-CD64 (10.1; BioLegend), 20 μg/ml anti-CD32A (IV.3; STEMCELL Technologies), 20 μg/ml isotype control (MPC-11; BioLegend), or 10 μg/ml isotype control (MOPC-21; BioLegend). Stimulation of Vα7.2$^+$ cells for 6 h with PMA/ionomycin (Leukocyte Activation Cocktail, with BD Golgi Plug; BD Biosciences) and in the presence of monensin was included in all experiments as a positive control. The different percentages were calculated as follows: cytokine expression boost (percentage) = [(cytokine$^+$ in the opsonized conditions − cytokine$^+$ in the nonopsonized conditions)/(cytokine$^+$ in the nonopsonized conditions)] × 100; response dependency (percentage) = [(cytokine$^+$ in presence of isotype control or without blocking − cytokine$^+$ in presence of the inhibitor)/(cytokine$^+$ in presence of isotype control or without blocking)] × 100; inhibition of cytokine expression boost with Fc fragment (percentage) = [(percentage boost without Fc fragment − percentage boost with Fc fragment)/(percentage boost without Fc fragment)] × 100.

Deglycosylation of IVIg

IVIg (GAMUNEX) were deglycosylated using Immobilized GlycINATOR (Genovis) as per the manufacturer's instructions. Deglycosylated IVIg was then used to opsonize *E. coli* as described above.

Soluble cytokine analysis

Supernatant from the MAIT cell activation assay was harvested after 24 h of stimulation and stored at −80°C before LEGENDplex (BioLegend) analysis following the manufacturer's instructions.

Phagocytosis assay

The monocytic cell line THP-1 was cultured in medium without FCS for 2 h prior to addition of *E. coli*. Bacteria were washed once in PBS, fixed in 1% formaldehyde for 3 min, vortexed during the first minute, and extensively washed in PBS. The bacteria were incubated in pHrodo Red dye at 0.05 mM (Thermo Fisher Scientific) and $NaHCO_3$ buffer at 100 mM for 30 min at 37°C. After washing in $NaHCO_3$ buffer, bacteria were opsonized with 5 mg/ml IVIg (GAMUNEX) for 30 min at 37°C or resuspended in medium without FCS. After extensive washes, the microbes were resuspended in medium without FCS and fed to THP-1 cells at the microbial dose of 1 for 3 h. THP-1 cells were then stained with LIVE/DEAD Fixable Near-IR dye (Invitrogen), fixed in 1% formaldehyde, and analyzed by flow cytometry.

Analysis of the MR1 Ag presentation pathway

The monocytic cell line THP-1 was cultured in RPMI 1640 without folic acid (Life Technologies) for 2 h prior to incubation with *E. coli* D21, *ribA*-deficient BSV-18 or 1100-2 nonopsonized or IVIg opsonized as described above with slight modification. After fixation and opsonization, the bacteria were resuspended in RPMI 1640 without folic acid and added to the THP-1 culture at the microbial dose of 100. After up to 4 h incubation, the cells were stained and fixed. In some experiments, THP-1 cells were preincubated 30 min with 5 μg/ml brefeldin A (Abcam), 20 μg/ml cytochalasin D (Sigma-Aldrich), 50 nM bafilomycin A (Sigma-Aldrich), 6.25 nM wortmannin (Sigma-Aldrich), 2.5 μM R406 (BioVision), 10 μg/ml anti-CD64 (10.1; BioLegend), 20 μg/ml anti-CD32A (IV.3; STEMCELL Technologies), 20 μg/ml isotype control (MPC-11; BioLegend), or 10 μg/ml isotype control (MOPC-21; BioLegend). In the wash conditions, THP-1 cells were preincubated 30 min before adding *E. coli* with the chemical inhibitors, then washed and supplemented with fresh RPMI 1640 without folic acid or with complete medium before continuing with the experiment.

Flow cytometry

Cell surface and intracellular staining was performed as previously described (15, 47). The Abs used were as follows: anti-CD3 Bv650 (OKT3; BioLegend), anti-CD3 FITC (SK7; BD Biosciences), anti-Vα7.2 PE (3C10; BioLegend), anti-CD161 Pe-Cy5 (DX12; BD Biosciences), anti-CD4 Bv711 (OKT4; BioLegend), anti-CD8 Bv570 (RPA-T8; BioLegend), anti-CD69 BUV737 (FN50; BD Biosciences), anti-CD107a BUV395 (H4A3; BD Biosciences), anti-GzB FITC (GB11; BioLegend), anti–IFN-γ allophycocyanin (25723.11; BD Biosciences), anti-TNF PE-Cy7 (Mab11; BD Biosciences), anti–IL-17A Bv421 (BL168; BioLegend), anti-RORγt allophycocyanin (R&D Systems), anti-RORγt Bv650 (Q21-559; BD Biosciences), anti-PLZF PECF594 (R17-809; BD Biosciences), anti–T-bet Bv711 or Bv605 (4B10; BioLegend), anti-MR1 (26.5; BioLegend), anti–HLA-DR (L243; BioLegend), anti–HLA-A2 (BB7.2; Bio-Rad Laboratories), LIVE/DEAD Fixable Aqua and Near-IR dye (Invitrogen). Flow cytometry data were acquired on BD LSRFortessa or BD FACSymphony A5 instruments (both BD Biosciences) and analyzed using FlowJo software v. 10.5.3 (Tree Star). Analyses of MAIT cell polyfunctionality were performed using the SPICE software v. 6.0 (48).

Statistics

Statistical analysis was performed using the Prism software v.7 (GraphPad). Data sets were first subjected to a data normality distribution test. Differences between groups of samples were analyzed for statistical significance using an unpaired *t* test or Mann–Whitney *U* test for unpaired data and a paired *t* test or Wilcoxon signed-rank test for paired data. Possible correlations in data sets were determined using Spearman rank correlation. Two-sided p values <0.05 were called significant.

Data availability

The data reported in this paper will be available upon request from the corresponding author.

Results

IgG opsonization enhances the magnitude of MR1-dependent MAIT cell responses to E. coli

To investigate whether MAIT cell responses to bacteria are modulated by opsonization, we incubated magnetic bead–purified $V\alpha7.2^+$ cells with THP-1 cells fed mildly fixed, nonopsonized, or IgG-opsonized *E. coli* and analyzed MAIT cell expression of cytokines and cytotoxic molecules by intracellular flow cytometry. In all functional assays, MAIT cells were identified as $V\alpha7.2^+CD161^+$ T cells (46). *E. coli* serves in this study as a model micro-organism with potent production of riboflavin metabolite Ags for presentation by MR1 (46). As a source of IgG against a commonly occurring antigenic microbe, such as *E. coli*, we used the pooled human serum IgG preparation IVIg. After 24 h of coculture, IVIg-opsonized *E. coli* stimulation induced a higher magnitude of IFN-γ, TNF, and IL-17A production in MAIT cells, as well as increased expression of the cytolytic effector molecule granzyme B (GzB) with concomitant degranulation (CD107a), as compared with nonopsonized *E. coli* (Fig. 1A, 1B). Interestingly, Bánki et al. (49) recently observed a similar increase in IFN-γ and TNF production in response to *E. coli* preincubated with IVIg. The increase in IFN-γ, TNF, and IL-17A production was confirmed by measuring their concentrations in the supernatant of the MAIT cell–THP-1 coculture (Fig. 1C).

MAIT cells are found in many barrier tissues, in which they are well positioned to respond to microbial infections. To investigate whether responses from MAIT cells in tissue can be similarly enhanced by IgG opsonization, we magnetic bead–purified $V\alpha7.2^+$ cells from tonsil tissue and stimulated these cells with THP-1 cells fed mildly fixed, nonopsonized, or IgG-opsonized *E. coli* (Supplemental Fig. 1A, 1B). Tonsil MAIT cells mounted only weak responses to nonopsonized *E. coli*, whereas IVIg-opsonized *E. coli* stimulation induced a higher magnitude of IFN-γ and IL-17A production in MAIT cells as well as increased degranulation and expression of GzB.

Ag-dependent activation of MAIT cells occurs when MR1-loaded Ags are recognized by the MAIT cell TCR, and such triggering is associated with TCR downregulation (45). IVIg-opsonized *E. coli* stimulation provoked enhanced downregulation of the Vα7.2 TCR in MAIT cells from blood compared with the nonopsonized stimulation (Supplemental Fig. 1C, 1D), with a similar pattern for tonsillar MAIT cells (Supplemental Fig. 1E). To assess to what extent the MAIT cell response was dependent on TCR triggering, we blocked the interaction between MR1 and the TCR by adding anti-MR1 Ab during the coculture. MAIT cell activation was highly dependent on MR1 recognition for both nonopsonized and IVIg-opsonized *E. coli* conditions (Fig. 1D, Supplemental Fig. 1F). However, the level of MR1 dependency was higher in the IVIg-opsonized conditions, suggesting a role for enhanced Ag presentation in the increased MAIT cell activation by opsonized bacteria.

Some MAIT cell functions can be activated by cytokines produced by APCs, including IL-12 and IL-18. Neutralization of IL-12p70 and IL-18 with mAbs during the MAIT cell assay inhibited MAIT cell cytokine production at a rate that differed between the functions tested (Fig. 1D). Interestingly, responses to opsonized *E. coli* displayed a lower dependency on IL-12 and IL-18 for IFN-γ and GzB secretion, as well as CD107a degranulation, compared with the nonopsonized stimulation (Fig. 1D). Unexpectedly, neutralization of IL-12p70 led to increased production of TNF, suggesting a possible inhibitory role of IL-12 on TNF production (Fig. 1D). GzB production in response to opsonized *E. coli* was nearly completely independent of IL-12 and IL-18 (Fig. 1D). Triple blocking of MR1, IL-12p70, and IL-18 potently inhibited MAIT cell expression of IFN-γ and TNF as well as CD107a degranulation (Fig. 1E). The GzB response was only

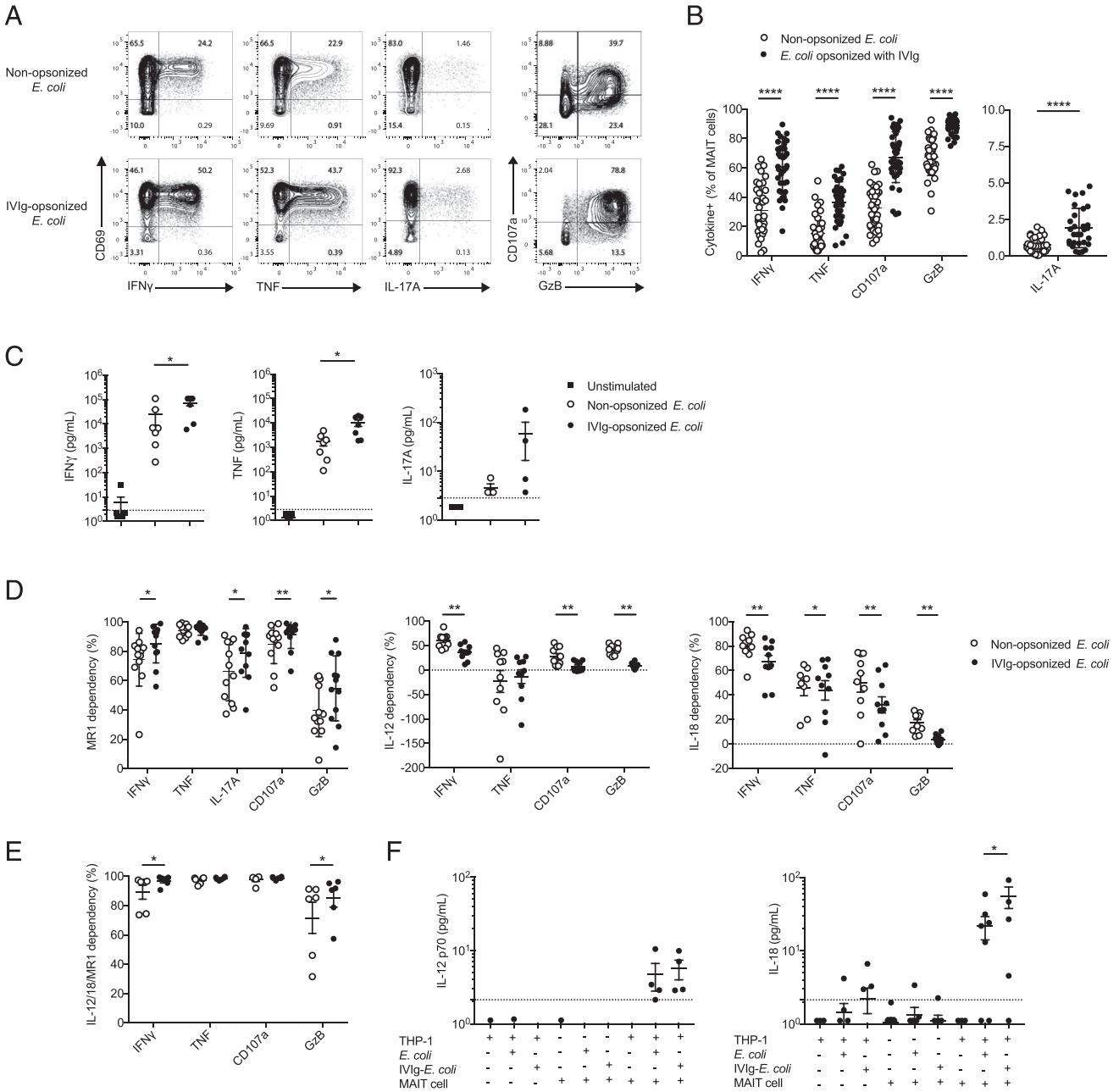

FIGURE 1. IgG-opsonization increases the magnitude of the MR1-restricted MAIT cell response to *E. coli*. Representative flow cytometry data (**A**), and mean percentage (**B**) of expression of IFN-γ, TNF, IL-17A, CD69, CD107a, and GzB in Vα7.2^{+}CD161^{+} MAIT cells stimulated for 24 h with THP-1 cells fed nonopsonized or IVIg-opsonized *E. coli* at the microbial dose of 1 (n = 30–38). (**C**) Concentration of IFN-γ, TNF, and IL-17A in the supernatant of the coculture after stimulation with nonopsonized and IVIg-opsonized *E. coli* for 24 h (n = 4–7). (**D**) MR1 and IL-12/IL-18 dependency of IFN-γ, TNF, IL-17A, CD107a, and GzB production. (**E**) MR1/IL-12/IL-18 dependency of IFN-γ, TNF, CD107a, and GzB production (n = 30–38). (**F**) Concentration of IL-12p70 and IL-18 in the supernatant of the 24-h coculture (n = 4–7). n = individual human donor cells tested in independent experiments. The lines and error bars represent mean and SE. In (D), response dependency (percentage) = ([cytokine^{+} in presence of isotype control or without blocking − cytokine^{+} in presence of blocking)/(cytokine^{+} in presence of isotype control or without blocking)] × 100. *$p < 0.05$, **$p < 0.005$, ****$p < 0.0001$ by the paired t test to determine significant differences between paired samples in (B) and (D) (left graph). *$p < 0.05$, **$p < 0.01$. and the Wilcoxon signed-rank test to detect significance in (C), [(D), center and right graph], (E), and (F).

partially blocked, revealing that other factors probably play a role in stimulation of GzB production by MAIT cells. It is interesting to note that the supernatant of the coculture of THP-1 cells fed IVIg-opsonized *E. coli* displayed a slightly higher concentration of IL-12p70 and a three-log increase in IL-18 compared with the nonopsonized condition (Fig. 1F). Notably, IVIg-opsonized *E. coli* was taken up more readily by THP-1 cells, as determined by intracellular detection by fluorescent pHrodo Red staining (Supplemental Fig. 1G, 1H). Taken together, these findings indicate that the MAIT cell response to *E. coli* is greatly enhanced in magnitude by preopsonization of the bacterium with IgG, mainly in an MR1-dependent manner, with a reduced dependency on cytokine costimulation.

MAIT cells responding to opsonized bacteria display increased polyfunctionality and enhanced T-bet expression

The repertoire of functions deployed by a T cell in response to stimulation can be more important than the magnitude of the

response. We therefore investigated the polyfunctionality of the MAIT cell response to nonopsonized or IVIg-opsonized microbes using SPICE software analysis (48). The MAIT cell polyfunctional profile differed between the two conditions, with a clear increase of MAIT cells responding with two, three, or four functions after stimulation with THP-1 cells fed IVIg-opsonized bacteria (Fig. 2A). This reflected a major increase of $GzB^+IFN\text{-}\gamma^+TNF^+$ and $GzB^+IFN\text{-}\gamma^+$ MAIT cells (Fig. 2B, 2C). We next determined the expression of key transcription factors in MAIT cells during these stimulatory conditions. The levels of T-bet increased in MAIT cells stimulated with IVIg-opsonized *E. coli* compared with the nonopsonized condition, whereas levels of RORγt and PLZF remained similar (Fig. 2D, 2E). A similar pattern was evident in MAIT cells from tonsils stimulated under the same conditions (data not shown). Thus, the MAIT cell response to IgG-opsonized bacteria is not only stronger but also qualitatively more complex.

Amplification of both sensitivity and kinetics of MAIT cell activation by IgG opsonization of E. coli

In the context of an infection, both the speed and sensitivity of Ag detection can be very important to limit microbial spread and provide effective protection of the host. Therefore, we next investigated the impact of IgG opsonization on sensitivity and kinetics of the MAIT cell response. Opsonization of *E. coli* increased the dose sensitivity leading to higher IFN-γ production by MAIT cells at suboptimal doses of bacteria (Fig. 3A). This effect was amplified along with the concentration of IVIg used for opsonization. The Vα7.2 TCR downregulation followed a similar pattern (Fig. 3A), indicative of enhanced Ag presentation and TCR triggering following IVIg-opsonized *E. coli* stimulation. Expression of TNF and GzB, as well as CD107a degranulation, displayed similar dose sensitivity–response curves (Supplemental Fig. 2A).

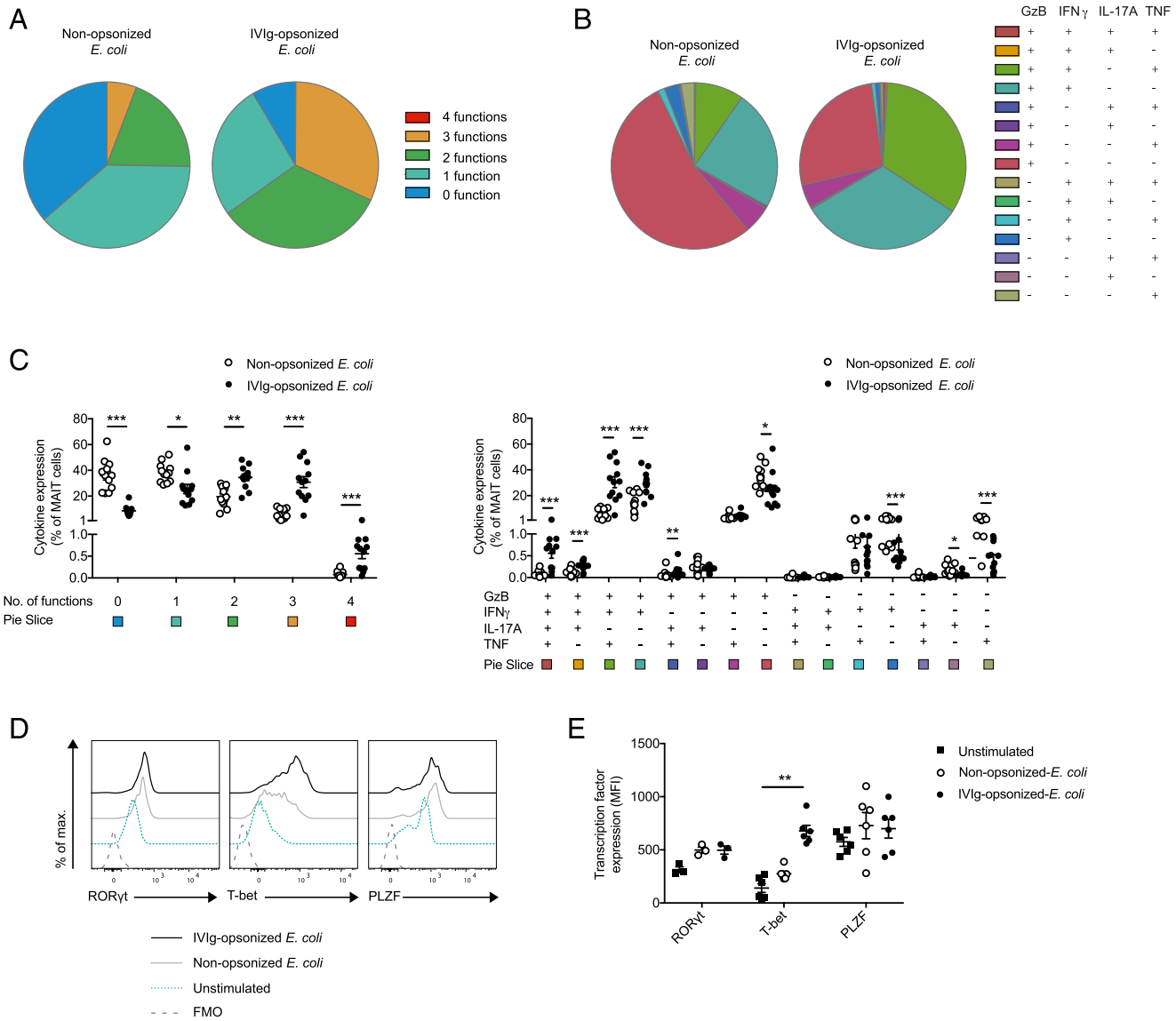

FIGURE 2. MAIT cell polyfunctionality and T-bet expression are increased by IVIg-opsonized *E. coli* stimulation. Polyfunctional profile of $V\alpha7.2^+CD161^+$ MAIT cells responding to nonopsonized or IgG-opsonized *E. coli* in terms of the number of functions displayed (**A**), and combinations of IFN-γ, TNF, IL-17A, and GzB production (**B**). (A)–(**C**) show the frequency of MAIT cells expressing all combinations of functions or cytokines ($n = 12$). Representative flow cytometry histograms (**D**), and combined data and ratio (**E**) of RORγt, T-bet, and PLZF expression in MAIT cells unstimulated or in the presence of nonopsonized or IVIg-opsonized *E. coli* for 24 h ($n = 3$–6). The fluorescence minus one (FMO) control is showed as gray dashed line in (D). The lines and error bars represent mean and SE. $^*p < 0.05$, $^{**}p < 0.01$, $^{***}p < 0.001$ by the Wilcoxon signed-rank test to detect significance in (C). $^*p < 0.05$, $^{**}p < 0.005$ by the Friedman test followed by Dunn post hoc test to determine significant differences between multiple, paired samples in (E).

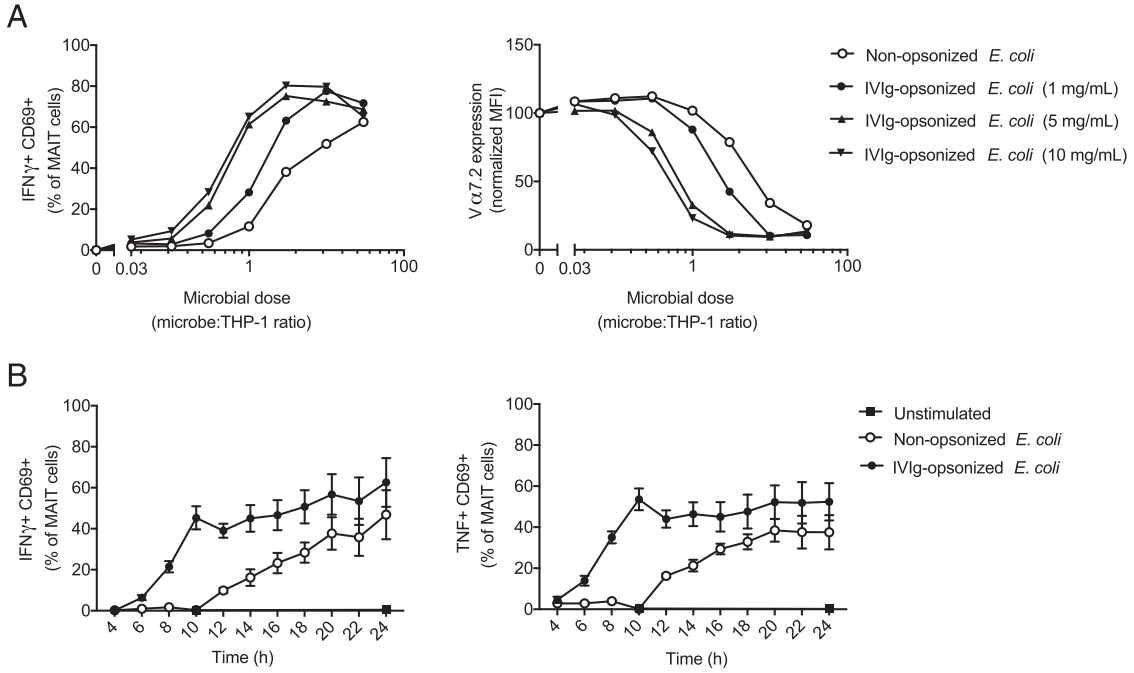

FIGURE 3. MAIT cell responses to IgG-opsonized *E. coli* display enhanced dose sensitivity and kinetics. (**A**) Percentage of IFN-γ^+CD69$^+$ and relative normalized Vα7.2 expression in Vα7.2$^+$CD161$^+$ MAIT cells stimulated by THP-1 cells fed nonopsonized or IVIg-opsonized *E. coli* over a range of microbial doses and at different concentrations of IVIg. Data shown representative of five independent experiments. (**B**) Percentage of IFN-γ^+CD69$^+$ and TNF$^+$ MAIT cells over 24 h of incubation, with MAIT cell harvest every 2 h (n = 3). The lines and error bars represent mean and SE.

To assess the effect of opsonization on the kinetics of MAIT cell responses to bacteria, we next performed a time-kinetic assay using the optimal 5 mg/ml IVIg opsonization dose. Within 10 h, the MAIT cell IFN-γ and TNF production following the IVIg-opsonized *E. coli* stimulation reached the level of cytokines produced by MAIT cells stimulated with the nonopsonized bacteria after 24 h of stimulation (Fig. 3B). The pattern was similar for CD107a degranulation, whereas GzB production and Vα7.2 downregulation occurred earlier and at a greater magnitude in the IVIg-opsonized conditions (Supplemental Fig. 2B). Altogether, these findings suggest that opsonization accelerates MAIT cell recognition of microbial Ags and lowers the threshold of activation of MAIT cell effector functions.

Enhancement of MAIT cell responses to IgG-opsonized E. coli *requires APC–FcγR binding*

The enhanced ability of THP-1 cells incubated with opsonized bacteria to activate MAIT cells suggests enhanced Ag uptake and loading via FcγR engagement. To test this possibility, we blocked FcγR by incubating THP-1 cells with human IgG Fc fragments prior to addition of the bacteria. In the presence of soluble Fc fragments, the MAIT cell IgG opsonization response boost was strongly inhibited (Fig. 4A, 4B, Supplemental Fig. 3A). The inhibition was ~80% for IFN-γ, TNF, and CD107a and 50% for GzB (Fig. 4C). Similarly, Fc fragment–mediated blocking inhibited TCR triggering, as evidenced by the weaker Vα7.2 TCR downregulation (Supplemental Fig. 3A). THP-1 cells express FcγRI and FcγRII (50), and therefore, to assess the potential involvement of these receptors in the enhanced Ag presentation to MAIT cells, we blocked FcγRI and FcγRIIA with anti-CD64 and anti-CD32A mAbs, respectively. Blocking the high-affinity receptor CD64 diminished TNF expression, CD107a degranulation, and Vα7.2 downregulation in the IVIg-stimulated conditions (Supplemental Fig. 3B, 3C). On the contrary, blocking CD32A had no detectable effect (Supplemental Fig. 3D).

Ig glycosylation is important for binding of IgG to FcγR (51). EndoS2 is an endoglycosidase from *S. pyogenes*, which hydrolyzes *N*-linked glycans on the IgG Fc part and reduces its binding to the FcγR (52). To further investigate this aspect of FcγR involvement, we used EndoS2 to deglycosylate IVIg before use in the opsonization assay. MAIT cell responses to *E. coli* opsonized using deglycosylated IVIg were similar to the nonopsonized condition (Fig. 4D, 4E), indicating that glycan-dependent binding of IVIg to the FcγR is required for the downstream enhancement of MAIT cell responses. The production of IL-17A and GzB, as well as CD107a degranulation and Vα7.2 TCR downregulation, followed a similar pattern (Supplemental Fig. 3E). Altogether, these data demonstrate that Fc-dependent engagement of FcγRs by the IVIg-opsonized *E. coli* is crucial for the enhancement of MAIT cell responses by IgG opsonization of the stimulating microbe.

Enhanced MR1-mediated Ag presentation via FcγR signaling, uptake, and ER transport

At steady state, MR1 molecules are retained in an incompletely folded conformation inside the ER with very low or undetectable levels at the cell surface. Once Ag is bound, the MR1–Ag complex translocates to the cell surface, where it can be recognized by MAIT cells (28). Thus, upregulation of MR1 surface expression can function as an indicator of MR1 ligand availability and loading. To assess how opsonization may affect these processes, we evaluated MR1 cell surface expression after exposure to nonopsonized and IVIg-opsonized bacteria. After incubation with IVIg-opsonized *E. coli*, MR1 cell surface expression levels were significantly enhanced, as compared with incubation with nonopsonized *E. coli* (Fig. 5A, 5B). In contrast, surface levels of MHC class I remained stable, and levels of MHC class II were just modestly increased, for both nonopsonized and opsonized conditions. Kinetics of MR1 expression under these conditions showed that the increase provoked by opsonized bacteria was not immediate,

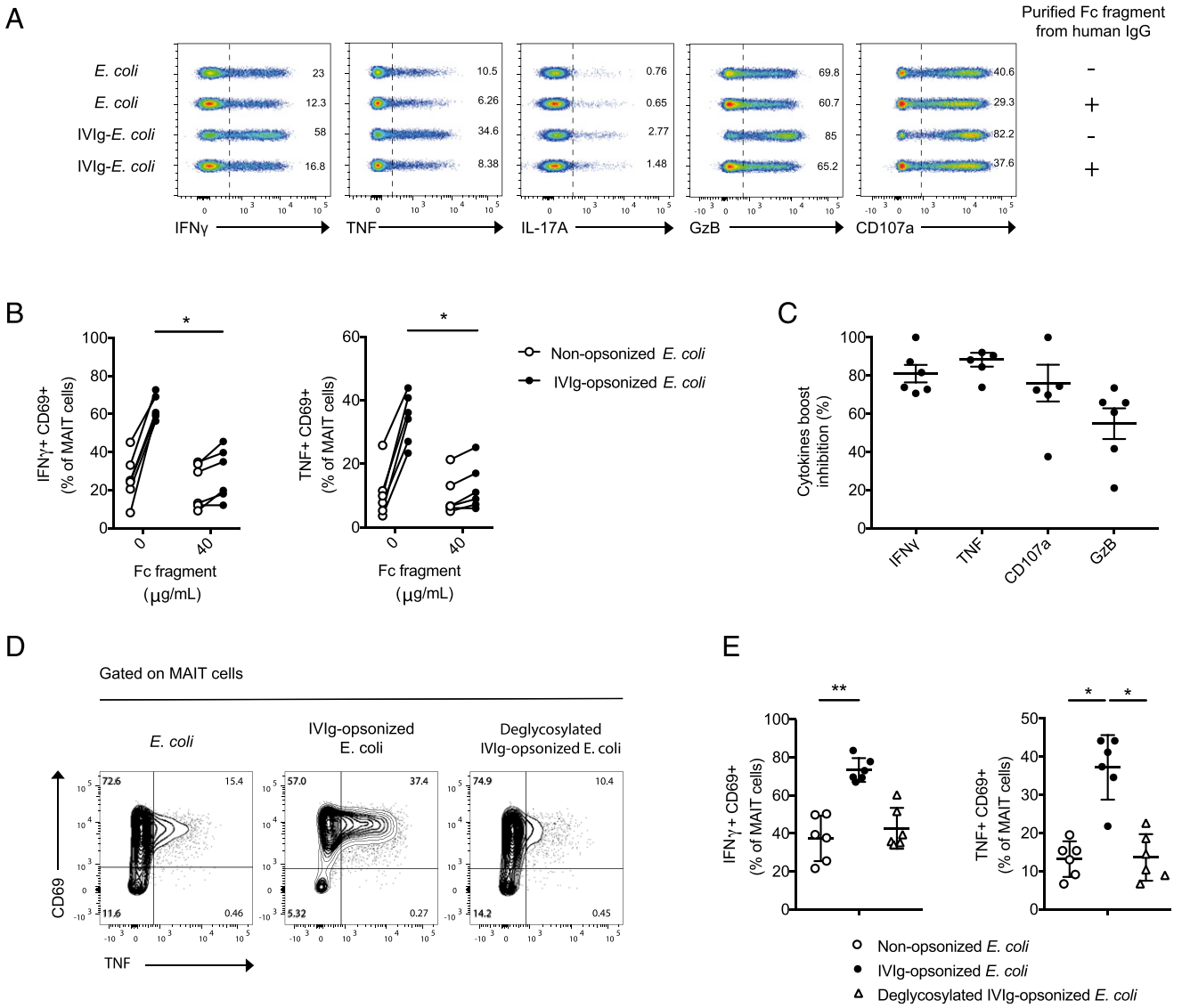

FIGURE 4. Enhanced MAIT cell responses to IgG-opsonized bacteria are dependent on FcγR binding. Representative flow cytometry data of the expression of IFN-γ, TNF, IL-17A, GzB, and CD107a (**A**), and percentage of IFN-γ^+CD69$^+$ and TNF$^+$CD69$^+$ MAIT cells (**B**) in the presence of THP-1 cells fed nonopsonized or IVIg-opsonized *E. coli* and with or without purified Fc fragment for 24 h ($n = 6$). (**C**) Percentage of the boost inhibition because of the Fc fragment for the indicated cytokines. Representative example of TNF and CD69 expression (**D**) and percentage of IFN-γ^+CD69$^+$ and TNF$^+$CD69$^+$ MAIT cells (**E**) in the presence of THP-1 cells fed nonopsonized, IVIg-opsonized, or deglycosylated IVIg-opsonized *E. coli* ($n = 6$). The lines and error bars represent mean and SE. $^*p < 0.05$ by the Wilcoxon signed-rank test performed to detect significance in (B). $^*p < 0.05$, $^{**}p < 0.005$ by the Friedman test followed by Dunn post hoc test to determine significant differences between multiple, paired samples in (C) and (E).

and the cells needed at least 3 h to express high levels of MR1 on their surface (Fig. 5C).

To determine which pathways were involved in the enhancement of MR1 expression, we targeted different key components of Ag processing using chemical inhibitors (Fig. 5D). Cytochalasin D, an inhibitor of actin polymerization that disrupts cytoskeleton assembly and therefore phagocytosis, strongly inhibited the increase in MR1 expression at the cell surface. Because unloaded MR1 molecules are retained as a pool in the ER, blockade of ER egress was assessed with brefeldin A, which strongly inhibited cell surface expression of MR1. Further, upregulation of MR1 expression was partially inhibited by bafilomycin A1, suggesting that passage in a lysosomal compartment is involved in the enhancement of MR1 expression at the cell surface induced by IVIg-opsonized bacteria. Next, we targeted the spleen tyrosine kinase (Syk), an early signaling protein that transmits signals from the ITAM of the activating FcγR CD32A or the FcRγ adaptor protein associated with CD16A and CD64. The Syk inhibitor R406 strongly inhibited MR1 surface upregulation induced by IVIg-opsonized bacteria. Similarly, wortmannin blocking of class IA PI3K, involved downstream of Syk in FcγR signaling, repressed MR1 surface expression (Supplemental Fig. 4A). Finally, blocking the FcγR with IgG Fc fragment prevented the increase in MR1 cell surface expression (Fig. 5D). Specific blocking of FcγR with anti-CD64 reduced MR1 cell surface expression, whereas anti-CD32 blocking slightly increased MR1 expression (Supplemental Fig. 4A). Incubation of THP-1 cells with IVIg-opsonized BSV-18, a *ribA*-deficient *E. coli* strain unable to synthesize riboflavin (45, 53), did not lead to increased MR1 surface expression (Supplemental Fig. 4B). In contrast, the IVIg-opsonized congenic riboflavin synthesis-competent 1100-2 strain induced an augmented MR1 cell surface expression as expected. Taken together, these findings indicate that FcγR signaling is a key event in the increased MR1 Ag loading in response to IgG-opsonized *E. coli*, supporting enhanced

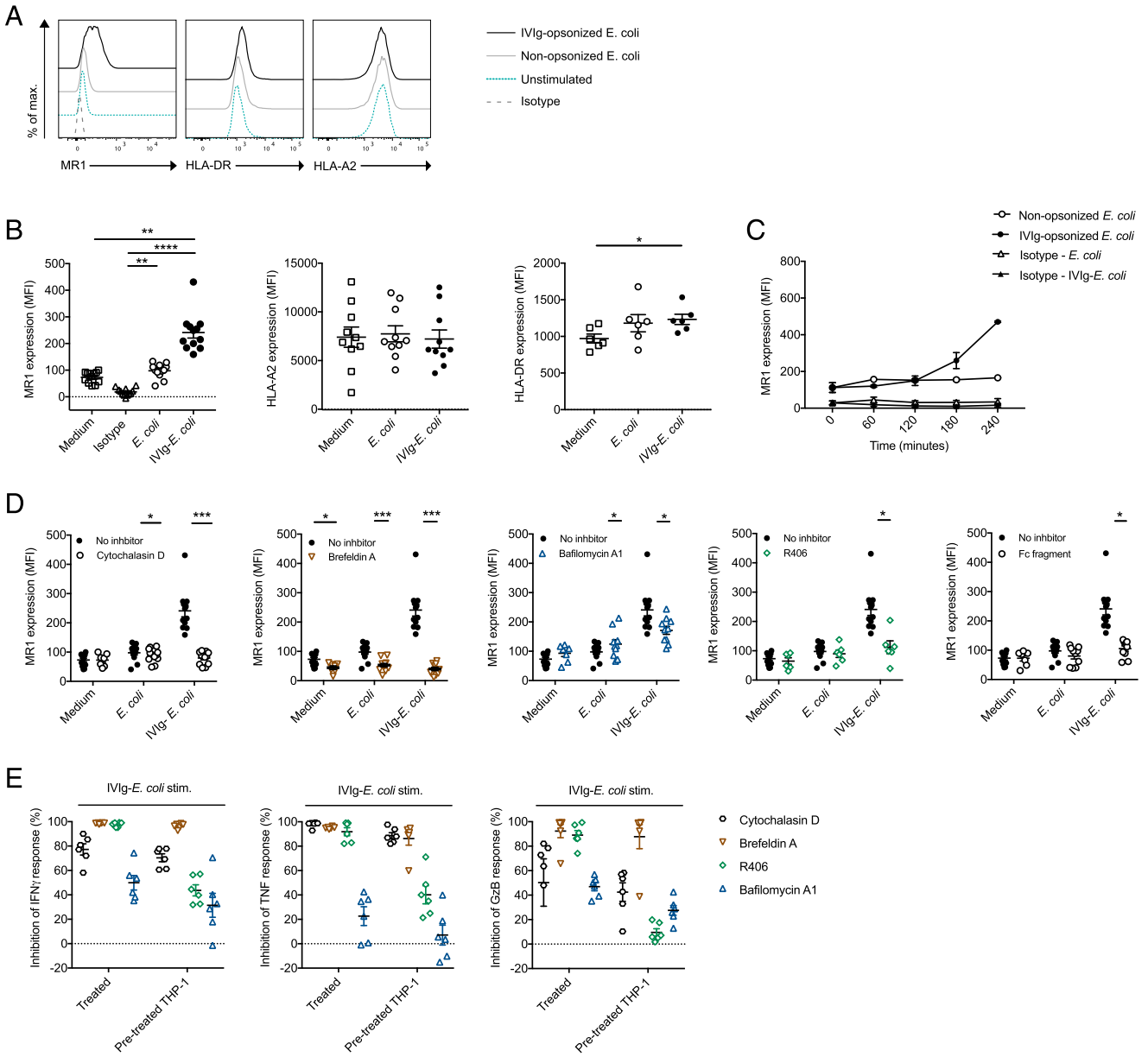

FIGURE 5. Increase in MR1-mediated Ag presentation by IVIg-opsonized bacteria is dependent on bacterial uptake, MR1 ER egress, and lysosomal acidification. Representative flow cytometry histogram (**A**), and combined donor data (**B**) on MR1, HLA-DR, and HLA-A2 expression in THP-1 cells fed with nonopsonized or IVIg-opsonized *E. coli* for 3 h ($n = 6–12$). The MR1 isotype control staining is shown as gray dashed line in (A). (**C**) Kinetics of MR1 expression on THP-1 cells in presence of nonopsonized or IVIg-opsonized *E. coli*. The MR1 isotype control staining is shown for both stimulations ($n = 2–4$). (**D**) MR1 expression in THP-1 cells unstimulated or in the presence of nonopsonized or IVIg-opsonized *E. coli* and with indicated compound for 3 h ($n = 6–12$). (**E**) The degree of inhibition of the MAIT cell response stimulated by IVIg-opsonized *E. coli* for 24 h, in presence of the indicated compound. For the THP-1 wash conditions, THP-1 cells were incubated for 30 min in presence of the compound, then washed, resuspended in fresh medium, and cocultured with MAIT cells for 24 h. The lines and error bars represent mean and SE. $*p < 0.05$, $**p < 0.005$, $****p < 0.0001$ by the Friedman test followed by Dunn post hoc test to detect significant differences between multiple, paired samples in (B). $*p < 0.05$, $***p < 0.001$ by the Wilcoxon signed-rank test to determine significance in (D).

Ag delivery to an MR1-containing endosomal compartment or ER or triggering signals that bring the pool of MR1 out of the ER to encounter the Ag.

We next investigated how downstream MAIT cell cytokine responses were affected by inhibiting these pathways in THP-1 cells (Fig. 5E). Presence of cytochalasin D, brefeldin A, or R406 almost completely inhibited MAIT cell production of IFN-γ or TNF and, to a lower extent, GzB upregulation, whereas bafilomycin A1 had a partial effect (Fig. 5E). To control for direct effects of these inhibitors on MAIT cells, we included an additional experimental condition in which THP-1 cells were pretreated for 30 min and washed carefully before addition of MAIT cells to the assay. The effects of cytochalasin D and brefeldin A on MAIT cell responses in this assay were still clear, whereas the effect of R406 was less distinct but still evident. Altogether, these findings indicate that APC bacterial uptake, FcγR triggering, and ER transport are required for IgG-mediated enhancement of Ag presentation and hence for increased MAIT cell responses to IVIg-opsonized *E. coli*.

Sera from humans vaccinated against S. pneumoniae *enhance MAIT cell recognition of this pathogen*

S. pneumoniae is a Gram-positive bacterium and opportunistic pathogen. We analyzed serum samples of healthy adults taken

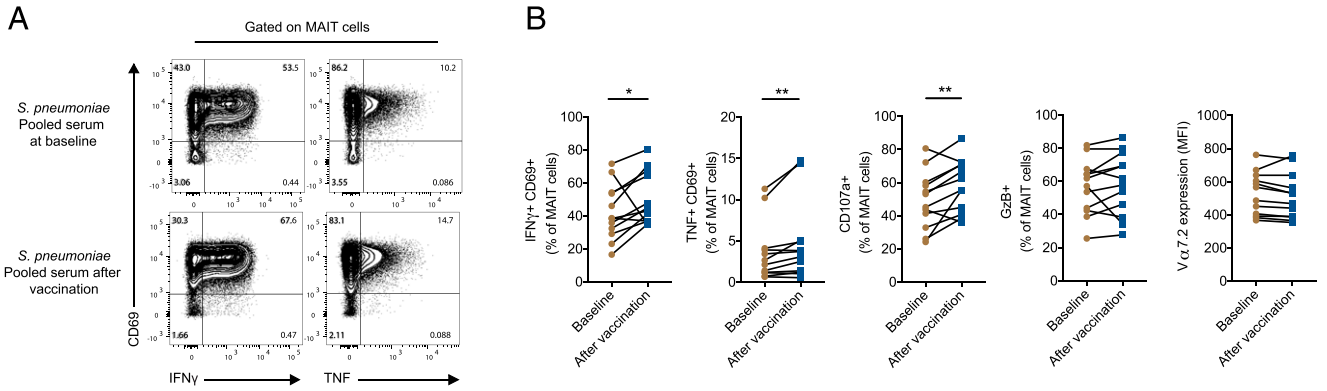

FIGURE 6. Sera from human subjects after vaccination with the 13-valent *S. pneumoniae* vaccine support enhanced MAIT cell activation. Representative flow cytometry plots (**A**) of IFN-γ, TNF, and CD69 expression and combined data (**B**) of MAIT cell responses determined as percentage IFN-γ$^+$CD69$^+$, TNF$^+$CD69$^+$, CD107a$^+$, GzB$^+$, and mean fluorescence intensity (MFI) of the Vα7.2 TCR in Vα7.2$^+$CD161$^+$ MAIT cells in the presence of THP-1 cells incubated with sera-opsonized *S. pneumoniae* for 24 h (n = 12). *$p < 0.05$, **$p < 0.01$ by the Wilcoxon signed-rank test to determine significance in (B).

before and after vaccination with Prevnar13, a 13-valent–conjugated vaccine directed against 13 different serotypes of *S. pneumoniae* in a previously published clinical trial (44). Pooled sera from the nine healthy vaccine recipients were used to opsonize *S. pneumoniae* 19A, one of the 13 strains included in the vaccine. MAIT cell stimulation with *S. pneumoniae* 19A opsonized with sera drawn after vaccination displayed increased IFN-γ and TNF expression as well as elevated CD107a degranulation compared with stimulation with *S. pneumoniae* opsonized with the serum collected from the same donors before vaccination (Fig. 6). Furthermore, there was a significant positive correlation between the percentage increase in OPA and the enhancement of MAIT cell TNF expression by opsonization and also between the 19A-specific IgG serum titer increase and the boost of CD107a expression by serum-opsonized bacteria (Table I). The increase in MAIT cell function against *S. pneumoniae* was MR1 dependent, as blocking Ag presentation with the MR1 antagonist acetyl-6-formylpterin (54) decreased IFN-γ and TNF production (Supplemental Fig. 4C). Taken together, these results suggest that Ag-specific Abs raised by vaccination may enhance MAIT cell responses to *S. pneumoniae*.

Discussion

MAIT cells are unconventional innate-like T cells present in all healthy humans (1–4). The frequency in circulation differs widely between donors, and the normal healthy range is from ∼0.5% up to 15% of all T cells (5). MAIT cells recognize Ag presented by the nonpolymorphic MR1 molecules, and this means that they can play critical roles in human immune defense and can potentially be therapeutically mobilized to treat infections in a donor-unrestricted fashion, without previous Ag-specific priming. In this study, we explored the interplay between MAIT cells and the humoral immune response and show that Abs against the model microbe *E. coli* can efficiently enhance the sensitivity, kinetics, and quality of MAIT cell recognition of this bacterium. Conversely, these findings also mean that MAIT cells can act as an effector arm of humoral immunity and deploy their full range of effector functions much more efficiently if a microbe is targeted and opsonized for uptake and processing by IgG. Given the size of the MAIT cell pool and their significant tissue-resident presence in sites, such as the liver and the lung, we speculate that this interplay with humoral immunity can be an important aspect of human immune defense against many microbes. Our finding that vaccination-induced Abs against *S. pneumoniae* enhance MAIT cell responses to this bacterium suggests that the MAIT cell–IgG axis is relevant in the context of pneumococcal disease.

In the normal healthy state, when cells are not infected or exposed to bacteria producing MR1-binding riboflavin metabolite Ags, MR1 is mostly located intracellularly in the ER and endosomal compartments, with very low levels on the cell surface. Our data show that uptake of IgG-opsonized *E. coli* leads to significant MR1 surface upregulation in THP-1 cells. This observation indicates that the FcγR-mediated uptake supports more efficient Ag processing and loading into MR1 molecules for transport to the cell surface. Previous studies indicated that Ag loading into MR1 occurs primarily in the ER, and that binding of the short-lived riboflavin metabolite Ags is needed to release MR1 from the ER (28). Our data showing almost complete block of Ag presentation by brefeldin A in both IgG-opsonized and nonopsonized conditions is consistent with a need for ER egress of MR1 molecules in this process. However, whether ER is the site of Ag loading is not clear from our data. Inhibition of endosomal acidification and of Syk signaling also partly impaired MR1 Ag presentation in THP-1 cells after exposure to IgG-opsonized *E. coli*, suggesting that the Ag processing and loading process is complex and involves several compartments.

The enhanced MR1 Ag presentation of IgG-opsonized *E. coli* caused MAIT cell responses of higher magnitude, a finding supported by similar observations by Bánki et al. (49). More importantly, however, we found that IgG opsonization allowed MAIT cells to respond with much faster kinetics and with efficient detection of lower doses of bacteria. The higher dose sensitivity and more rapid detection is probably more important than the response magnitude,

Table I. Correlations between titers, opsonization data, and MAIT cell functions

	OPA Increase (%)		Titer Increase (%)	
Cytokine	r	p	r	p
IFN-γ	0.55	0.1328	0.3333	0.3853
TNF	0.7333	**0.0311**	0.5	0.1777
CD107a	0.4	0.2912	0.7167	**0.0369**
GzB	0.4667	0.2125	0.4	0.2912

Nonparametric Spearman correlation between the percentage of cytokine expression enhancement in MAIT cells, the percentage of OPA increase, and the percentage of 19A-IgG titer increase (n = 9). r = Spearman correlation coefficient. For each of the nine serum donors, 4–11 MAIT cell donors were tested in the opsonization assay. The median of the percentage cytokine expression enhancement was calculated for each serum donor and used for the correlation calculation. Numbers in bold indicate statistically significant differences, $p < 0.05$.

per se, in the setting of the acute stages of a bacterial infection. The ability to detect lower bacterial loads sooner may be a deciding factor for the outcome of the host immune response, in particular, as MAIT cells are numerous and their response is more readily available without the several days of clonal expansion often required for an adaptive T cell response to mount. In the vaccine setting, it is possible that T cell–independent vaccines that generate humoral immunity could engage MAIT cells in this way. Interestingly, MAIT cells have also been found to provide T cell help for Ab production by B cells (53).

An important aspect of our results is that the IgG-opsonized *E. coli* Ag presentation drives a MAIT cell response that displays a higher level of polyfunctionality. In particular, we observed an increased prevalence of three- and four-functional profiles, with $GzB^+IFN\text{-}\gamma^+TNF^+$, $GzB^+IFN\text{-}\gamma^+$, and $GzB^+IFN\text{-}\gamma^+TNF^+IL\text{-}17^+$ combinations increasing, whereas monofunctional response profiles were less common. It is possible that the higher density of antigenic MR1 complexes causes stronger TCR signaling, in turn leading to enhancement of these polyfunctional response patterns. The enhanced TCR downregulation observed in response to IgG-opsonized *E. coli* is consistent with this hypothesis. Previous data from studies of adaptive antiviral CD8 T cell responses indicate that polyfunctionality is an important aspect of the quality and protective capacity of T cell responses (55) and that this may be linked with the level of Ag sensitivity (56). Another interesting difference between MAIT cells responding to nonopsonized and IgG-opsonized *E. coli* is that the IgG-opsonized condition leads to stronger upregulation of T-bet in the responding MAIT cells. It is notable that the augmentation of T-bet expression in MAIT cells stimulated with IgG-opsonized bacteria occurs alongside their increased expression of GzB, indicative of cytolytic arming of the cells.

Several infectious and noninfectious conditions are associated with decline or depletion of the MAIT cell compartment. These include, for example, acquired immunodeficiency in chronic HIV-1 infection (57, 58) and patients with primary immunodeficiency in common variable immunodeficiency (59). MAIT cells also decline during normal human aging (60). Furthermore, partial MAIT cell deficiency has been described in patients with STAT3 mutations (61), and recently, a case with severe MAIT cell deficiency was associated with extreme susceptibility to lung infections (62). The IgG-dependent enhancement of MAIT cell responses we have described in this study may thus be impaired in patients with immunodeficiency and in the elderly. In fact, a lack of specific Abs against pathogenic bacteria or decreased levels of MAIT cells may worsen the outcome of bacterial infections. However, we show in this study that it is possible to boost MAIT cell responses by vaccine-induced pneumococcus-specific IgG, thus underscoring the clinical potential of our findings. In this context, approaches to restore and expand MAIT cells in vivo could be important. Wang et al. (23) demonstrated enhanced protection against *L. longbeachae* in mice after adoptive transfer of MAIT cells or vaccination with MAIT cell–activating ligand. In humans, a pilot study of IL-7 treatment was shown to expand MAIT cells in HIV-1–infected patients on antiretroviral treatment (63).

In summary, we show significant enhancement of human MAIT cell responses to clinically important bacterial species via IgG-mediated opsonization. Ags from the opsonized bacteria are more efficiently processed and presented on MR1 molecules at the cell surface, leading to stronger, faster, and more sensitive triggering of MAIT cell responses with more complex qualitative characteristics. These findings show significant interplay between humoral immunity and the innate-like MAIT cells that may be important for immune protection of the host, both in the setting of bacterial infection and for vaccination strategies for patient groups at risk for pneumococcal infections.

Acknowledgments

The *S. pneumoniae* 1344 19A strain was a kind gift from Dr. Birgitta Henriques-Normark.

Disclosures

The authors have no financial conflicts of interest.

References

1. Toubal, A., I. Nel, S. Lotersztajn, and A. Lehuen. 2019. Mucosal-associated invariant T cells and disease. *Nat. Rev. Immunol.* 19: 643–657.
2. Dias, J., C. Boulouis, M. J. Sobkowiak, K. G. Lal, J. Emgård, M. Buggert, T. Parrot, J. B. Gorin, E. Leeansyah, and J. K. Sandberg. 2018. Factors influencing functional heterogeneity in human mucosa-associated invariant T cells. *Front. Immunol.* 9: 1602.
3. Gherardin, N. A., J. McCluskey, J. Rossjohn, and D. I. Godfrey. 2018. The diverse family of MR1-restricted T cells. *J. Immunol.* 201: 2862–2871.
4. Provine, N. M., and P. Klenerman. 2020. MAIT cells in health and disease. *Annu. Rev. Immunol.* 38: 203–228.
5. Dusseaux, M., E. Martin, N. Serriari, I. Péguillet, V. Premel, D. Louis, M. Milder, L. Le Bourhis, C. Soudais, E. Treiner, and O. Lantz. 2011. Human MAIT cells are xenobiotic-resistant, tissue-targeted, CD161hi IL-17-secreting T cells. *Blood* 117: 1250–1259.
6. Martin, E., E. Treiner, L. Duban, L. Guerri, H. Laude, C. Toly, V. Premel, A. Devys, I. C. Moura, F. Tilloy, et al. 2009. Stepwise development of MAIT cells in mouse and human. *PLoS Biol.* 7: e54.
7. Treiner, E., L. Duban, S. Bahram, M. Radosavljevic, V. Wanner, F. Tilloy, P. Affaticati, S. Gilfillan, and O. Lantz. 2003. Selection of evolutionarily conserved mucosal-associated invariant T cells by MR1. [Published erratum appears in 2003 *Nature* 423: 1018.] *Nature* 422: 164–169.
8. Tilloy, F., E. Treiner, S. H. Park, C. Garcia, F. Lemonnier, H. de la Salle, A. Bendelac, M. Bonneville, and O. Lantz. 1999. An invariant T cell receptor alpha chain defines a novel TAP-independent major histocompatibility complex class Ib-restricted alpha/beta T cell subpopulation in mammals. *J. Exp. Med.* 189: 1907–1921.
9. Walker, L. J., Y. H. Kang, M. O. Smith, H. Tharmalingham, N. Ramamurthy, V. M. Fleming, N. Sahgal, A. Leslie, Y. Oo, A. Geremia, et al. 2012. Human MAIT and CD8αα cells develop from a pool of type-17 precommitted CD8+ T cells. *Blood* 119: 422–433.
10. Lepore, M., A. Kalinichenko, A. Colone, B. Paleja, A. Singhal, A. Tschumi, B. Lee, M. Poidinger, F. Zolezzi, L. Quagliata, et al. 2014. Parallel T-cell cloning and deep sequencing of human MAIT cells reveal stable oligoclonal TCRβ repertoire. [Published erratum appears in 2014 *Nat. Commun.* 5: 4493.] *Nat. Commun.* 5: 3866.
11. Kjer-Nielsen, L., O. Patel, A. J. Corbett, J. Le Nours, B. Meehan, L. Liu, M. Bhati, Z. Chen, L. Kostenko, R. Reantragoon, et al. 2012. MR1 presents microbial vitamin B metabolites to MAIT cells. *Nature* 491: 717–723.
12. Corbett, A. J., S. B. Eckle, R. W. Birkinshaw, L. Liu, O. Patel, J. Mahony, Z. Chen, R. Reantragoon, B. Meehan, H. Cao, et al. 2014. T-cell activation by transitory neo-antigens derived from distinct microbial pathways. *Nature* 509: 361–365.
13. Le Bourhis, L., E. Martin, I. Péguillet, A. Guihot, N. Froux, M. Coré, E. Lévy, M. Dusseaux, V. Meyssonnier, V. Premel, et al. 2010. Antimicrobial activity of mucosal-associated invariant T cells. [Published erratum appears in 2010 *Nat. Immunol.* 11: 969.] *Nat. Immunol.* 11: 701–708.
14. Le Bourhis, L., M. Dusseaux, A. Bohineust, S. Bessoles, E. Martin, V. Premel, M. Coré, D. Sleurs, N. E. Serriari, E. Treiner, et al. 2013. MAIT cells detect and efficiently lyse bacterially-infected epithelial cells. *PLoS Pathog.* 9: e1003681.
15. Leeansyah, E., J. Svärd, J. Dias, M. Buggert, J. Nyström, M. F. Quigley, M. Moll, A. Sönnerborg, P. Nowak, and J. K. Sandberg. 2015. Arming of MAIT cell cytolytic antimicrobial activity is induced by IL-7 and defective in HIV-1 infection. *PLoS Pathog.* 11: e1005072.
16. Kurioka, A., J. E. Ussher, C. Cosgrove, C. Clough, J. R. Fergusson, K. Smith, Y. H. Kang, L. J. Walker, T. H. Hansen, C. B. Willberg, and P. Klenerman. 2015. MAIT cells are licensed through granzyme exchange to kill bacterially sensitized targets. *Mucosal Immunol.* 8: 429–440.
17. Trottein, F., and C. Paget. 2018. Natural killer T cells and mucosal-associated invariant T cells in lung infections. *Front. Immunol.* 9: 1750.
18. Chua, W. J., S. M. Truscott, C. S. Eickhoff, A. Blazevic, D. F. Hoft, and T. H. Hansen. 2012. Polyclonal mucosa-associated invariant T cells have unique innate functions in bacterial infection. *Infect. Immun.* 80: 3256–3267.
19. Gold, M. C., S. Cerri, S. Smyk-Pearson, M. E. Cansler, T. M. Vogt, J. Delepine, E. Winata, G. M. Swarbrick, W. J. Chua, Y. Y. Yu, et al. 2010. Human mucosal associated invariant T cells detect bacterially infected cells. *PLoS Biol.* 8: e1000407.
20. Georgel, P., M. Radosavljevic, C. Macquin, and S. Bahram. 2011. The non-conventional MHC class I MR1 molecule controls infection by *Klebsiella pneumoniae* in mice. *Mol. Immunol.* 48: 769–775.
21. Meierovics, A., W. J. Yankelevich, and S. C. Cowley. 2013. MAIT cells are critical for optimal mucosal immune responses during in vivo pulmonary bacterial infection. *Proc. Natl. Acad. Sci. USA* 110: E3119–E3128.

22. Meierovics, A. I., and S. C. Cowley. 2016. MAIT cells promote inflammatory monocyte differentiation into dendritic cells during pulmonary intracellular infection. *J. Exp. Med.* 213: 2793–2809.
23. Wang, H., C. D'Souza, X. Y. Lim, L. Kostenko, T. J. Pediongco, S. B. G. Eckle, B. S. Meehan, M. Shi, N. Wang, S. Li, et al. 2018. MAIT cells protect against pulmonary *Legionella* longbeachae infection. *Nat. Commun.* 9: 3350.
24. Rouxel, O., J. Da Silva, L. Beaudoin, I. Nel, C. Tard, L. Cagninacci, B. Kiaf, M. Oshima, M. Diedisheim, M. Salou, et al. 2017. Cytotoxic and regulatory roles of mucosal-associated invariant T cells in type 1 diabetes. [Published erratum appears in 2018 *Nat. Immunol.* 19: 1035.] *Nat. Immunol.* 18: 1321–1331.
25. Riegert, P., V. Wanner, and S. Bahram. 1998. Genomics, isoforms, expression, and phylogeny of the MHC class I-related MR1 gene. *J. Immunol.* 161: 4066–4077.
26. Huang, S., E. Martin, S. Kim, L. Yu, C. Soudais, D. H. Fremont, O. Lantz, and T. H. Hansen. 2009. MR1 antigen presentation to mucosal-associated invariant T cells was highly conserved in evolution. *Proc. Natl. Acad. Sci. USA* 106: 8290–8295.
27. Tsukamoto, K., J. E. Deakin, J. A. Graves, and K. Hashimoto. 2013. Exceptionally high conservation of the MHC class I-related gene, MR1, among mammals. *Immunogenetics* 65: 115–124.
28. McWilliam, H. E., S. B. Eckle, A. Theodossis, L. Liu, Z. Chen, J. M. Wubben, D. P. Fairlie, R. A. Strugnell, J. D. Mintern, J. McCluskey, et al. 2016. The intracellular pathway for the presentation of vitamin B-related antigens by the antigen-presenting molecule MR1. *Nat. Immunol.* 17: 531–537.
29. Ussher, J. E., B. van Wilgenburg, R. F. Hannaway, K. Ruustal, P. Phalora, A. Kurioka, T. H. Hansen, C. B. Willberg, R. E. Phillips, and P. Klenerman. 2016. TLR signaling in human antigen-presenting cells regulates MR1-dependent activation of MAIT cells. *Eur. J. Immunol.* 46: 1600–1614.
30. Slichter, C. K., A. McDavid, H. W. Miller, G. Finak, B. J. Seymour, J. P. McNevin, G. Diaz, J. L. Czartoski, M. J. McElrath, R. Gottardo, and M. Prlic. 2016. Distinct activation thresholds of human conventional and innate-like memory T cells. *JCI Insight*. DOI: 10.1172/jci.insight.86292.
31. Loh, L., Z. Wang, S. Sant, M. Koutsakos, S. Jegaskanda, A. J. Corbett, L. Liu, D. P. Fairlie, J. Crowe, J. Rossjohn, et al. 2016. Human mucosal-associated invariant T cells contribute to antiviral influenza immunity via IL-18-dependent activation. *Proc. Natl. Acad. Sci. USA* 113: 10133–10138.
32. Ussher, J. E., M. Bilton, E. Attwod, J. Shadwell, R. Richardson, C. de Lara, E. Mettke, A. Kurioka, T. H. Hansen, P. Klenerman, and C. B. Willberg. 2014. CD161++ CD8+ T cells, including the MAIT cell subset, are specifically activated by IL-12+IL-18 in a TCR-independent manner. *Eur. J. Immunol.* 44: 195–203.
33. Dias, J., E. Leeansyah, and J. K. Sandberg. 2017. Multiple layers of heterogeneity and subset diversity in human MAIT cell responses to distinct microorganisms and to innate cytokines. *Proc. Natl. Acad. Sci. USA* 114: E5434–E5443.
34. Lal, K. G., D. Kim, M. C. Costanzo, M. Creegan, E. Leeansyah, J. Dias, D. Paquin-Proulx, L. A. Eller, A. Schuetz, Y. Phuang-Ngern, et al. 2020. Dynamic MAIT cell response with progressively enhanced innateness during acute HIV-1 infection. *Nat. Commun.* 11: 272.
35. Gordon, S. 2016. Phagocytosis: an immunobiologic process. *Immunity* 44: 463–475.
36. Guilliams, M., P. Bruhns, Y. Saeys, H. Hammad, and B. N. Lambrecht. 2014. The function of Fcγ receptors in dendritic cells and macrophages. [Published erratum appears in 2014 *Nat. Rev. Immunol.* 14: 349.] *Nat. Rev. Immunol.* 14: 94–108.
37. Bournazos, S., T. T. Wang, R. Dahan, J. Maamary, and J. V. Ravetch. 2017. Signaling by antibodies: recent progress. *Annu. Rev. Immunol.* 35: 285–311.
38. Weiser, J. N., D. M. Ferreira, and J. C. Paton. 2018. *Streptococcus pneumoniae*: transmission, colonization and invasion. *Nat. Rev. Microbiol.* 16: 355–367.
39. Kim, D. K., C. B. Bridges, and K. H. Harriman, Centers for Disease Control and Prevention (CDC), Advisory Committee on Immunization Practices (ACIP), ACIP Adult Immunization Work Group. 2015. Advisory committee on immunization practices recommended immunization schedule for adults aged 19 years or older--United States, 2015. *MMWR Morb. Mortal. Wkly. Rep.* 64: 91–92.
40. Wilson, R., J. M. Cohen, M. Reglinski, R. J. Jose, W. Y. Chan, H. Marshall, C. de Vogel, S. Gordon, D. Goldblatt, F. C. Petersen, et al. 2017. Naturally acquired human immunity to pneumococcus is dependent on antibody to protein antigens. [Published erratum appears in 2017 *PLoS Pathog.* 13: e1006259.] *PLoS Pathog.* 13: e1006137.
41. Moberley, S., J. Holden, D. P. Tatham, and R. M. Andrews. 2013. Vaccines for preventing pneumococcal infection in adults. *Cochrane Database Syst. Rev.*: CD000422.
42. Kurioka, A., B. van Wilgenburg, R. R. Javan, R. Hoyle, A. J. van Tonder, C. L. Harrold, T. Leng, L. J. Howson, D. Shepherd, V. Cerundolo, et al. 2018. Diverse *Streptococcus pneumoniae* strains drive a mucosal-associated invariant T-cell response through major histocompatibility complex class I-related molecule-dependent and cytokine-driven pathways. *J. Infect. Dis.* 217: 988–999.
43. Hartmann, N., C. McMurtrey, M. L. Sorensen, M. E. Huber, R. Kurapova, F. T. Coleman, J. P. Mizgerd, W. Hildebrand, M. Kronenberg, D. M. Lewinsohn, and M. J. Harriff. 2018. Riboflavin metabolism variation among clinical isolates of *Streptococcus pneumoniae* results in differential activation of mucosal-associated invariant T cells. *Am. J. Respir. Cell Mol. Biol.* 58: 767–776.
44. Zangenah, S., L. Björkhem-Bergman, A. C. Norlin, S. Hansen, L. Lindqvist, B. Henriques-Normark, and P. Bergman. 2017. The pneumocell-study: vaccination of IgG1- and IgG2-deficient patients with Prevnar13. *Vaccine* 35: 2654–2660.
45. Dias, J., C. Boulouis, J. B. Gorin, R. H. G. A. van den Biggelaar, K. G. Lal, A. Gibbs, L. Loh, M. Y. Gulam, W. R. Sia, S. Bari, et al. 2018. The $CD4^{-}CD8^{-}$ MAIT cell subpopulation is a functionally distinct subset developmentally related to the main $CD8^{+}$ MAIT cell pool. *Proc. Natl. Acad. Sci. USA* 115: E11513–E11522.
46. Dias, J., M. J. Sobkowiak, J. K. Sandberg, and E. Leeansyah. 2016. Human MAIT-cell responses to *Escherichia coli*: activation, cytokine production, proliferation, and cytotoxicity. *J. Leukoc. Biol.* 100: 233–240.
47. Dias, J., J. K. Sandberg, and E. Leeansyah. 2017. Extensive phenotypic analysis, transcription factor profiling, and effector cytokine production of human MAIT cells by flow cytometry. *Methods Mol. Biol.* 1514: 241–256.
48. Roederer, M., J. L. Nozzi, and M. C. Nason. 2011. SPICE: exploration and analysis of post-cytometric complex multivariate datasets. *Cytometry A* 79: 167–174.
49. Bánki, Z., L. Krabbendam, D. Klaver, T. Leng, S. Kruis, H. Mehta, B. Müllauer, D. Orth-Höller, H. Stoiber, C. B. Willberg, and P. Klenerman. 2019. Antibody opsonization enhances MAIT cell responsiveness to bacteria via a TNF-dependent mechanism. *Immunol. Cell Biol.* 97: 538–551.
50. Fleit, H. B., and C. D. Kobasiuk. 1991. The human monocyte-like cell line THP-1 expresses Fc gamma RI and Fc gamma RII. *J. Leukoc. Biol.* 49: 556–565.
51. Nimmerjahn, F., and J. V. Ravetch. 2008. Fcgamma receptors as regulators of immune responses. *Nat. Rev. Immunol.* 8: 34–47.
52. Collin, M., and A. Olsén. 2001. EndoS, a novel secreted protein from *Streptococcus pyogenes* with endoglycosidase activity on human IgG. *EMBO J.* 20: 3046–3055.
53. Bennett, M. S., S. Trivedi, A. S. Iyer, J. S. Hale, and D. T. Leung. 2017. Human mucosal-associated invariant T (MAIT) cells possess capacity for B cell help. *J. Leukoc. Biol.* 102: 1261–1269.
54. Eckle, S. B., R. W. Birkinshaw, L. Kostenko, A. J. Corbett, H. E. McWilliam, R. Reantragoon, Z. Chen, N. A. Gherardin, T. Beddoe, L. Liu, et al. 2014. A molecular basis underpinning the T cell receptor heterogeneity of mucosal-associated invariant T cells. *J. Exp. Med.* 211: 1585–1600.
55. Betts, M. R., M. C. Nason, S. M. West, S. C. De Rosa, S. A. Migueles, J. Abraham, M. M. Lederman, J. M. Benito, P. A. Goepfert, M. Connors, et al. 2006. HIV nonprogressors preferentially maintain highly functional HIV-specific CD8+ T cells. *Blood* 107: 4781–4789.
56. Almeida, J. R., D. Sauce, D. A. Price, L. Papagno, S. Y. Shin, A. Moris, M. Larsen, G. Pancino, D. C. Douek, B. Autran, et al. 2009. Antigen sensitivity is a major determinant of CD8+ T-cell polyfunctionality and HIV-suppressive activity. *Blood* 113: 6351–6360.
57. Leeansyah, E., A. Ganesh, M. F. Quigley, A. Sönnerborg, J. Andersson, P. W. Hunt, M. Somsouk, S. G. Deeks, J. N. Martin, M. Moll, et al. 2013. Activation, exhaustion, and persistent decline of the antimicrobial MR1-restricted MAIT-cell population in chronic HIV-1 infection. *Blood* 121: 1124–1135.
58. Cosgrove, C., J. E. Ussher, A. Rauch, K. Gärtner, A. Kurioka, M. H. Hühn, K. Adelmann, Y. H. Kang, J. R. Fergusson, P. Simmonds, et al. 2013. Early and nonreversible decrease of CD161++ /MAIT cells in HIV infection. *Blood* 121: 951–961.
59. Paquin-Proulx, D., B. A. N. Santos, N. S. Barsotti, A. K. B. B. Marinho, C. M. Kokron, K. I. Carvalho, M. T. Barros, J. Kalil, M. Elmacken, J. K. Sandberg, et al. 2017. Loss of circulating mucosal-associated invariant T cells in common variable immunodeficiency is associated with immune activation and loss of eomes and PLZF. *Immunohorizons* 1: 142–155.
60. Lee, O. J., Y. N. Cho, S. J. Kee, M. J. Kim, H. M. Jin, S. J. Lee, K. J. Park, T. J. Kim, S. S. Lee, Y. S. Kwon, et al. 2014. Circulating mucosal-associated invariant T cell levels and their cytokine levels in healthy adults. *Exp. Gerontol.* 49: 47–54.
61. Wilson, R. P., M. L. Ives, G. Rao, A. Lau, K. Payne, M. Kobayashi, P. D. Arkwright, J. Peake, M. Wong, S. Adelstein, et al. 2015. STAT3 is a critical cell-intrinsic regulator of human unconventional T cell numbers and function. *J. Exp. Med.* 212: 855–864.
62. Pincikova, T., D. Paquin-Proulx, M. Moll, M. Flodström-Tullberg, L. Hjelte, and J. K. Sandberg. 2018. Severely impaired control of bacterial infections in a patient with cystic fibrosis defective in mucosal-associated invariant T cells. *Chest* 153: e93–e96.
63. Sortino, O., E. Richards, J. Dias, E. Leeansyah, J. K. Sandberg, and I. Sereti. 2018. IL-7 treatment supports CD8+ mucosa-associated invariant T-cell restoration in HIV-1-infected patients on antiretroviral therapy. *AIDS* 32: 825–828.